ToF-SIMS and XPS Analysis of the Surface Chemical Structure of Some Linear Poly(orthoesters)

M. C. Davies* and R. A. P. Lynn

Department of Pharmaceutical Sciences, School of Pharmacy, University of Nottingham, Nottingham NG7 2RD, U.K.

J. F. Watts

Department of Materials Science and Engineering, University of Surrey, Guildford, Surrey GU2 5XH, U.K.

A. J. Paul and J. C. Vickerman

Centre for Surface and Materials Analysis, UMIST, Manchester M60 1QD, U.K.

J. Heller

Controlled Release and Biomedical Polymer Programme, SRI International, Menlo Park, California 94025

Received September 28, 1990; Revised Manuscript Received May 24, 1991

ABSTRACT: The surface chemical composition of a range of poly(orthoester) copolymers has been examined by using time-of-flight secondary ion mass spectrometry (ToF-SIMS) and X-ray photoelectron spectroscopy (XPS). A good correlation was observed between the theoretical and experimental elemental and chemical state data obtained by XPS. The ToF-SIMS spectra revealed a consistent fragmentation pattern throughout the copolymer series where ions detected were diagnostic of each repeat unit including high molecular weights diads and triads arising from the poly(orthoester) copolymer sequence. The intensity of the ions specific to the diols was shown to reflect the bulk composition in a quantitative manner. The nature of the fragmentation was interpreted in terms of cleavage of the ether bonds linking the diol and orthoester unit and through the endocyclic and exocyclic cleavage of the orthoester bonds.

Introduction

Over the last few decades, biodegradable polymer systems have attracted considerable interest for the controlled release of bioactive molecules.[1] A number of novel synthetic biodegradable polymer systems have been developed, most notable of which are the polyesters,[2] polyanhydrides,[3] and, of particular importance to this paper, the poly(orthoesters).[4] In each case, the polymer possesses a biodegradable functional group within the repeat unit, exhibits good biocompatibility, and displays programmable degradation kinetics.

The poly(orthoesters) have been shown to possess unique properties, which renders them suitable candidates for exploitation in advanced drug delivery. Poly(orthoesters) exhibit pH-sensitive surface degradation in the solid state, undergoing random chain scission in an acidic environment only. The addition of poorly soluble basic salts and acid anhydride excipients or the inclusion of an acidic functionality in the polymer structure influences the pH within the eroding surface gel layers.[5,6] Hence, the manipulation of the formulation to aid the development or inhibition of an acidic surface pH allows precise preprogramming of the polymer degradation process and, therefore, drug release rate. With the ability to vary the polymer composition together with the concentration and type of excipients, a range of poly(orthoesters) can be prepared, with degradation lifetimes varying from days to years.

The surface chemistry of these poly(orthoesters) is likely to play a major role in determining the in vivo performance of the polymers. The interfacial composition will not only dictate the biocompatibility exhibited by the host tissue to the implant but will also predetermine the kinetics of the surface degradation. While the poly(orthoester) bulk physicochemistry has been reported,[7] little information is available on the surface composition of these polymers.

SIMS has emerged as a complementary surface analysis technique to XPS, providing detailed molecular structure information for standard and biomedical polymers.[8–12] With specific reference to this work, SIMS has provided detailed surface structural information on biomedical (and in certain cases, biodegradable) polymers including the polyesters,[13] methacrylate-based copolymers,[14] polyurethanes,[15] and polyanhydrides.[16] However, the majority of reported studies on polymers have employed quadrupole-based mass spectrometers, with practical detection mass ranges of typically m/z 0–400. More recently, time-of-flight (ToF) instruments have been constructed that exhibit much higher transmission (>10% compared to 0.1%) than the quadrupole-based systems and parallel mass detection, both of which contribute to a considerable increase in sensitivity, with a typical effective mass range of m/z 0–10 000. Benninghoven, Hercules, and their respective co-workers have pioneered the application of ToF-SIMS for the analysis of a diverse range of standard and biomedical polymers.[17,18]

In this study, we report on the XPS and ToF-SIMS analysis of a series of poly(orthoesters) of the general formula given in Chart I. The polymers under examination were prepared by the addition of different proportions of two diols to the diketene acetal 3,9-diethylidene-2,4,8,-10-tetraoxaspiro[5.5]undecane (DETOSU), resulting in structures consisting of an alternating sequence of DETOSU and diol units. When varying ratios of the rigid diol *trans*-cyclohexanedimethanol (t-CDM) and the flexible diol 1,6-hexanediol (HD) (Table I) are used, random copolymers having different mechanical properties can be obtained. This procedure allows the preparation of materials having glass transition temperatures that can vary between about 120 °C and about 20 °C.

---

* Author to whom correspondence should be addressed.

0024-9297/91/2224-5508$02.50/0

Chart I

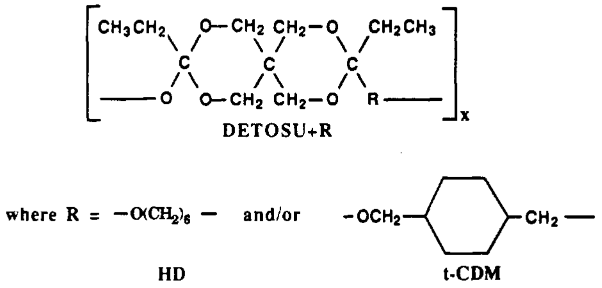

Table I
Polymer Compositions

polymer	composition, mol % DETOSU	CDM	HD
A	50	50	-
B	50	32.5	17.5
C	50	17.5	32.5
D	50	-	50

Experimental Section

Polymer Preparation and Film Formation. The synthesis of polymers was described previously.[4] Briefly, the desired ratio of *trans*-cyclohexanedimethanol and 1,6-hexanediol was added to tetrahydrofuran and the mixture stirred until all solids dissolved. A solution of the diketene acetal 3,9-diethylidene-2,4,8,10-tetraoxaspiro[5.5]undecane was then added and polymerization initiated by the addition of a catalytic amount of *p*-toluenesulfonic acid dissolved in tetrahydrofuran. After the initial exotherm subsided, the mixture was stirred for about 2 h and the polymer isolated by precipitation into a large excess of methanol containing a small amount of triethyleneamine stabilizer followed by filtration and vacuum drying at 60 °C for 24 h. Polymers prepared by this procedure typically have molecular weights in the 80–100-kDa range.

Polymer films for ToF-SIMS and XPS analysis were prepared by spin-casting onto acetone-washed aluminum foil from freshly prepared 0.1% w/v chloroform solutions.

Surface Analysis. XPS. XPS spectra were obtained by a VG Scientific ESCALAB Mk II electron spectrometer employing Mg Kα X-rays ($h\nu$ = 1253.6 eV). The X-ray gun was operated at 120 W, and spectra were recorded at an electron takeoff angle of 45°, corresponding to a depth analysis of about 5 nm. A survey scan spectrum (0–1000 eV) and narrow scans in the C 1s and O 1s regions were recorded for all samples. The analyzer was operated in a fixed transmission mode with a pass energy of 50 eV (for survey scans) and 20 eV (for C 1s and O 1s envelopes). Data acquisition and analysis were performed by a VGS 5000-S data system based on a DEC PDP 11/73 computer. The peak fitting of the O 1s and C 1s envelopes was performed by using methodology described elsewhere.[19] The recorded spectra were corrected for sample charging (referenced by C–H/*C*–C at 285 eV in the C 1s envelope). Quantification was achieved by using the manufacture's standard software supplied with the data system (VGS-5000S). The routine employed Scofield sensitivity factors corrected for the analyzer transmission function of the spectrometer.

ToF-SIMS. ToF-SIMS spectra were obtained by using a VG-Ionex IX23S instrument based on a Poschenrieder design and equipped with a pulsed liquid metal ion source.[20] A 30-keV Ga^+ primary ion beam was used at an incident angle of 38° to surface normal. The secondary ions were accelerated to ±5 keV for the analysis by applying a bias to the sample. The films, while continuous, were thin enough not to cause problems with sample charging, and therefore charge compensation with a pulsed electron flood gun was not required for the SIMS analysis. For each sample, both positive and negative secondary ion spectra were collected by using a total primary ion dose of 1×10^{11} ions cm^{-2}. Such a dose lies well below the damage threshold value of 1×10^{13} ions cm^{-2} for static SIMS.[21] A DEC PDP 11 computer system was used for spectral acquisition, storage, and data processing.

Table II
Elemental Composition[a] and C 1s Envelope Components from XPS

elem composition	polymer A	polymer B	polymer C	polymer D
C (T)	76.0	75.3	74.7	73.9
C (E)	77.2	76.2	75.8	73.9
O (T)	24.0	24.7	25.3	26.1
O (E)	22.8	23.8	24.2	26.1

% area under C 1s envelope	polymer A	polymer B	polymer C	polymer D
C–H/C–C (T)	47.4	45.4	43.5	41.2
(E)	49.0	46.0	43.0	44.0
C–CO_2–O (T)	10.5	10.9	11.3	11.8
(E)	10.0	11.0	12.0	11.0
C–O (T)	31.6	32.8	33.9	35.2
(E)	31.0	32.0	34.0	34.0
CO_2–O (T)	10.5	10.9	11.3	11.8
(E)	10.0	10.0	10.0	11.0

[a] Atomic percent excluding hydrogen. T = theoretical. E = experimental.

Results and Discussion

XPS. The XPS survey scans for all the poly(orthoesters) confirm the continuity and thickness (>5 nm) of the spin-cast films since signals from the underlying aluminum substrate were not detected. Carbon and oxygen only were detected in the survey scans, attesting to the elemental purity of these poly(orthoesters) within the XPS sensitivity levels (0.1%). The theoretical atomic percentages (excluding hydrogen) were calculated by examination of the structural formulas and are tabulated in Table II. Examination of the peak areas of the carbon and oxygen signals in the XPS spectra allows a quantitative elemental analysis of the polymer surfaces to be calculated and indicates that there is an extremely close correlation between the theoretical and experimental elemental data.

Four chemical states of carbon are fitted to each C 1s peak envelope. The major C 1s component in all the polymers corresponds to the *C*–C/*C*–H carbon environment at 285 eV. The carbon species at 286.6 eV corresponds to the ether carbon, i.e., *C*–O. The 289.2-eV peak may be assigned to the orthoester linkage, i.e., CO_2–O. A secondary chemical shift[22] was also fitted at 285.6 eV, corresponding to *C*–CO_2–O.

The experimental proportions of the four carbon environments are tabulated in Table II for the poly(orthoesters). There appears to be a very good correlation between these experimentally determined values and those anticipated from the structural formulas. Further confirmation of the surface chemical composition can be obtained from the O 1s signals at ~533 eV, which indicates the presence of only one oxygen environment (attributed to singly bonded oxygen).

ToF-SIMS. The positive ion ToF-SIMS spectra of the polymer series are shown for the mass ranges m/z 0–1000 and 1000–1500 in Figures 1–4 and 5, respectively. In Figure 5, the secondary ion signals above m/z 1000 recorded at low mass resolution were of low intensity and of confirmatory diagnostic value. In addition, no extraneous elemental or organic contamination was detected in the ToF-SIMS analysis of these polymers. This provides further evidence of the purity of the poly(orthoester) series. The fragmentation patterns of the polymers have been compared and analyzed in detail and for clarity; assignments of ions specific to each portion of the copolymer structure will be discussed separately.

Cations Diagnostic of DETOSU. Positive ions attributable to the orthoester monomer are observed as a diagnostic series in the m/z 100–300 range of Figures 1–4

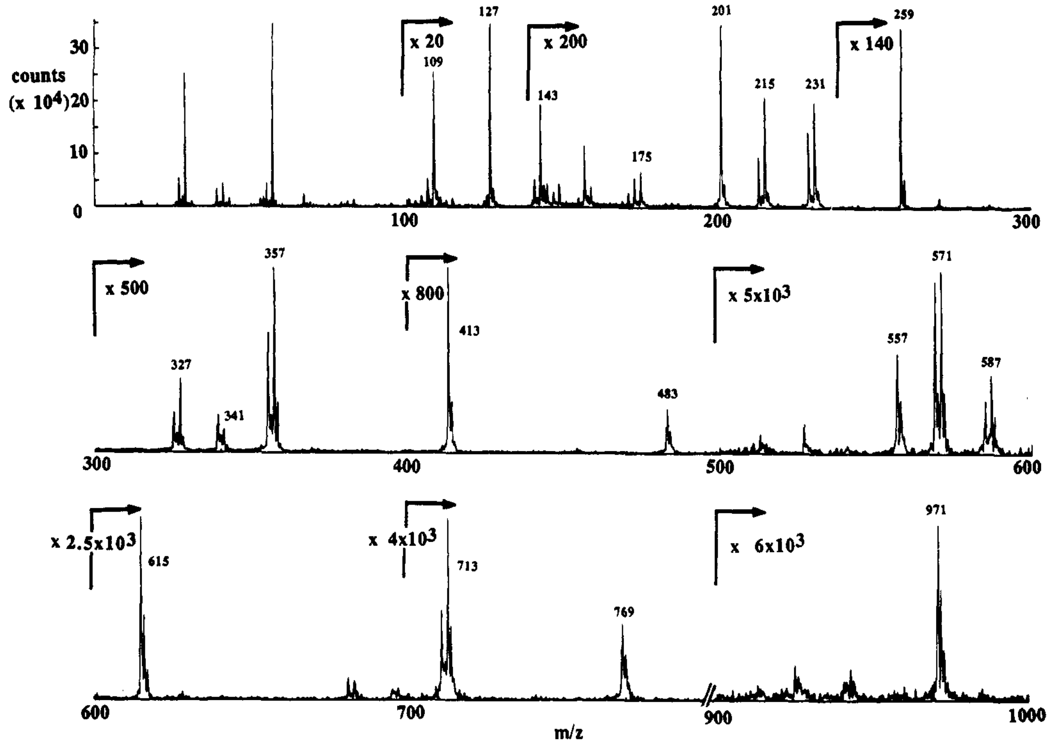

Figure 1. Positive ion ToF-SIMS spectrum of polymer A.

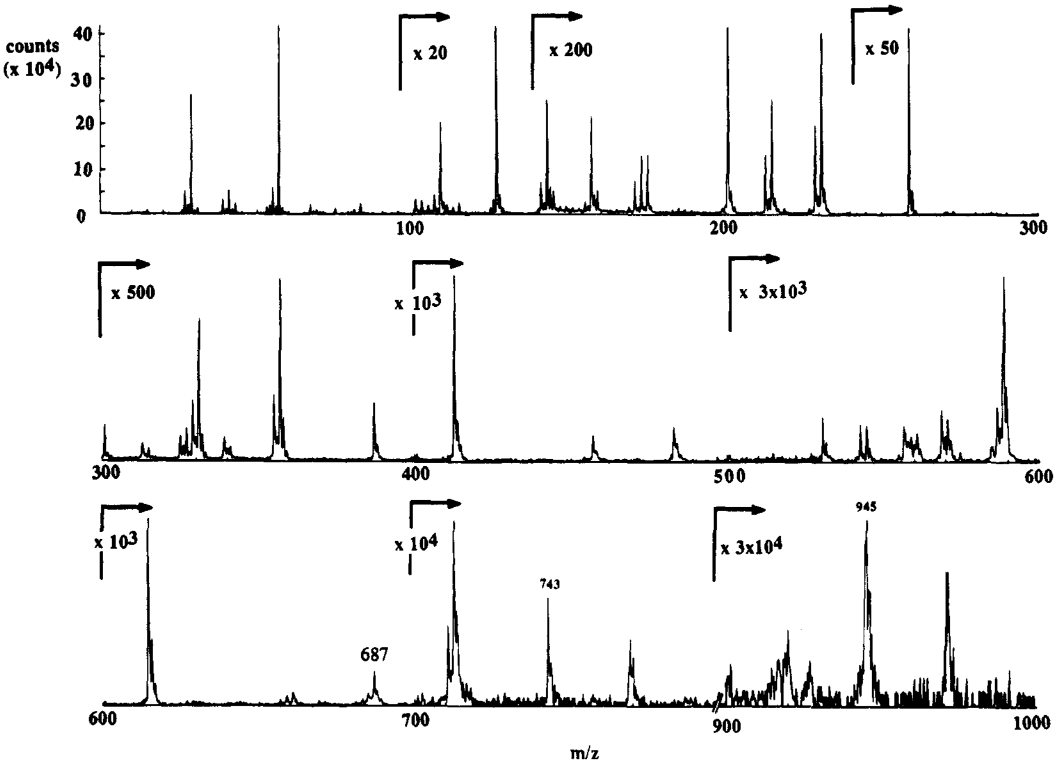

Figure 2. Positive ion ToF-SIMS spectrum of polymer B.

for all the polymers. Possible structures for some of the ions in this series are tabulated in Table III. Cations that may be assigned to structures derived from the intact monomer unit (where M is the mass of the monomer unit), i.e., $(M_{DETOSU} \pm H)^+$, $(M_{DETOSU} - O \pm H)^+$, and $(M_{DETOSU} - CH_2CH_3)^+$, are observed at *m/z* 231/229, 215/213, and 201, respectively. A dominant cation at *m/z* 259 is observed in all poly(orthoesters) examined. Separate ToF-SIMS and XPS studies on a range of poly(orthoesters) containing differing types of diols, and also the use of deuterated diols,[23] suggest that the *m/z* 259 ion is derived solely from the orthoester with no contribution from the diol. Similarly, the use of tandem quadrupole SIMS employing instrumentation and methodology described previously[26,27] to analyze the structure of the *m/z* 259 cation for a range of orthoesters did not reveal any further information. Thus, a structural assignment for this ion is not possible at present. We believe that the *m/z* 259 structure may also feature part of the higher mass diad and triad ions discussed in latter sections and noted in Tables IV–VI. Further fragments of the DETOSU unit may be assigned to the ions at *m/z* 175, 173, 159, 157, 143, and 127, as shown in Table III. These structures appear to be consistent with the cleavage of the copolymer chain and subsequent fragmentation in the region of the orthoester functional group.

Table III
Tentative Structural Assignments for Major Cations Derived from DETOSU

possible ion assignments	*m*/*z*	notation
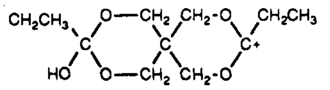	231	$(M + H)^+$
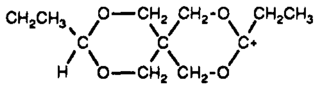	215	$(MH - O)^+$
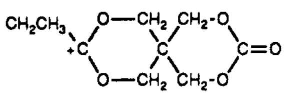	201	$(M - CH_2CH_3)^+$
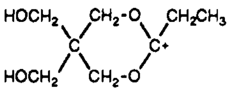	175 173 (i.e., −2 H)	
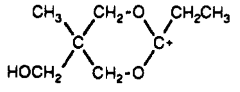	159 157 (i.e., −2 H)	
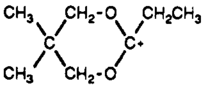	143	
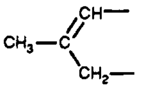 or 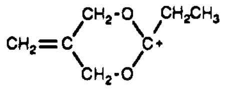	127	

Cations Diagnostic of the Diols HD and t-CDM. The contribution of the flexible and rigid diols to the ToF-SIMS spectra may be elucidated by the comparison of Figure 1 for polymer A and Figure 4 for polymer D. In the case of Figure 1, there is an intense *m*/*z* 109 cation that may be assigned to the following possible structures from the t-CDM unit with associated rearrangement of the initial primary carbonium ion

m/*z* 109

This *m*/*z* 109 ion is of very low intensity in Figure 4, and indeed the relative intensity decreases with Figure 1 to Figure 4, as anticipated from the change in the bulk polymer structure. With regard to cations specific to the HD flexible diol, signals at *m*/*z* 83, 101, and 103 are particularly intense in Figure 4 relative to Figure 1, and these may correspond to the following structures from the HD unit:

$$^+CH_2(CH_2)_3CH{=}CH_2 \quad m/z\ 83$$

$$^+(CH_2)_6OH \quad m/z\ 101$$

$$^+(H(CH_2)_6OH_2) \quad m/z\ 103$$

Again, these ions also appear to increase in their intensity from Figure 1 to Figure 4, in line with changes in the HD bulk copolymer content.

Cations Diagnostic of DETOSU + t-CDM. A number of prominent ions observed for polymer A in Figures 1 and 5a, and tabulated in Table IV, may be assigned to structures containing DETOSU repeat unit(s) attached to the CDM rigid diol unit(s) i.e., $[(M_{DETOSU} + M_{CDM})_n \pm H]^+$ where $n = 1$–4. Together with the detection of ions that may be assigned to intact multiple repeat units, a common pattern of ions is observed, which we suggest may be derived from the cleavage of bonds in the orthoester functional group, i.e., $(Y \pm H)^+$, $(Y - O \pm H)^+$, $(Y - CH_2CH_3)^+$, and $(Y + (C{=}O)CH_2CH_3)^+$, where Y represents a combination of one or more DETOSU and t-CDM repeat units. As anticipated, all these peaks are absent for polymer D in Figures 4 and 5d and, in general, show a relative decrease in intensity from Figure 1 to Figure 4 and from Figure 5a to Figure 5d, reflecting the changes in copolymer composition.

Table IV
Major Cations and Tentative Structural Assignments of the ToF-SIMS Analysis of Polymer A Shown in Figures 1 and 5a

m/*z*	assignment
327	$M_{DETOSU} + M_{CDM} - CH_2CH_3$
341/339	$M_{DETSOU} + M_{CDM} - O \pm H$
357/355	$M_{DETSOU} + M_{CDM} \pm H$
413	$M_{DETOSU} + M_{CDM} + (C{=}O)CH_2CH_3$
483	$M_{CDM} + M_{DETOSU}$ + structure y[a]
557	$M_{DETOSU} + M_{CDM} + M_{DETOSU} - CH_2CH_3$
571/569	$M_{DETOSU} + M_{CDM} + M_{DETOSU} - O \pm H$
587/585	$M_{DETOSU} + M_{CDM} + M_{DETOSU} \pm H$
615	$M_{DETOSU} + M_{CDM} + 259$[b]
683	$(M_{DETOSU} + M_{CDM})_2 - CH_2CH_3$
697/695	$(M_{DETOSU} + M_{CDM})_2 - O \pm H$
713/711	$(M_{DETOSU} + M_{CDM})_2 \pm H$
769	$(M_{DETOSU} + M_{CDM})_2 + (C{=}O)CH_2CH_3$
971	$(M_{DETOSU} + M_{CDM})_2 + 259$[b]
1039	$(M_{DETOSU} + M_{CDM})_3 - CH_2CH_3$
1051	$(M_{DETOSU} + M_{CDM})_3 - OH$
1069	$(M_{DETOSU} + M_{CDM})_3 + H$
1125	$(M_{DETOSU} + M_{CDM})_3 + (C{=}O)CH_2CH_3$
1327	$(M_{DETOSU} + M_{CDM})_3 + 259$[b]
1425	$(M_{DETOSU} + M_{CDM})_4 + H$
1481	$(M_{DETOSU} + M_{CDM})_4 + (C{=}O)CH_2CH_3$

[a] Structure y is equivalent to the structure assigned to the ion *m*/*z* 127 derived from DETOSU as shown in Table III. [b] The 259th component of the cation is equivalent to the ion derived from DETOSU as noted in the text.

Table V
Major Cations and Tentative Structural Assignments for ToF-SIMS Analysis of Polymer D Shown in Figures 4 and 5d

m/*z*	assignment
301	$M_{DETOSU} + M_{HD} - CH_2CH_3$
315/313	$M_{DETOSU} + M_{HD} - O \pm H$
331/329	$M_{DETOSU} + M_{HD} \pm H$
387	$M_{DETOSU} + M_{HD} + (C{=}O)CH_2CH_3$
457	$M_{DETOSU} + M_{HD}$ + structure y[a]
531	$M_{DETOSU} + M_{HD} + M_{DETOSU} - CH_2CH_3$
545/543	$M_{DETOSU} + M_{HD} + M_{DETOSU} - O \pm H$
559/561	$M_{DETOSU} + M_{HD} + M_{DETOSU} \pm H$
589	$M_{HD} + M_{DETOSU} + 259$[b]
631	$(M_{DETOSU} + M_{HD})_2 - CH_2CH_3$
643/645	$(M_{DETOSU} + M_{HD})_2 - O \pm H$
661/659	$(M_{DETOSU} + M_{HD})_2 \pm H$
717	$(M_{DETOSU} + M_{HD})_2 + (C{=}O)CH_2CH_3$
919	$(M_{DETOSU} + M_{HD})_2 + 259$[b]
989/991	$(M_{DETOSU} + M_{HD})_3 \pm H$
1047	$(M_{DETOSU} + M_{HD})_3 + (C{=}O)CH_2CH_3$
1249	$(M_{DETOSU} + M_{HD})_3 + 259$[b]
1321	$(M_{DETOSU} + M_{HD})_4 + H$
1377	$(M_{DETOSU} + M_{HD})_4 + (C{=}O)CH_2CH_3$

[a] Structure y is equivalent to the structure assigned to the ion *m*/*z* 127 derived from DETOSU as shown in Table III. [b] The 259th component of the cation is equivalent to the ion derived from DETOSU as noted in the text.

Cations Diagnostic of DETOSU + HD. Table V lists the diagnostic ions from the ToF-SIMS spectrum of polymer D in Figures 4 and 5d. The intensities of these ions noted in Table V gradually reduce from Figure 4 to Figure 2, being totally absent from the ToF-SIMS spec-

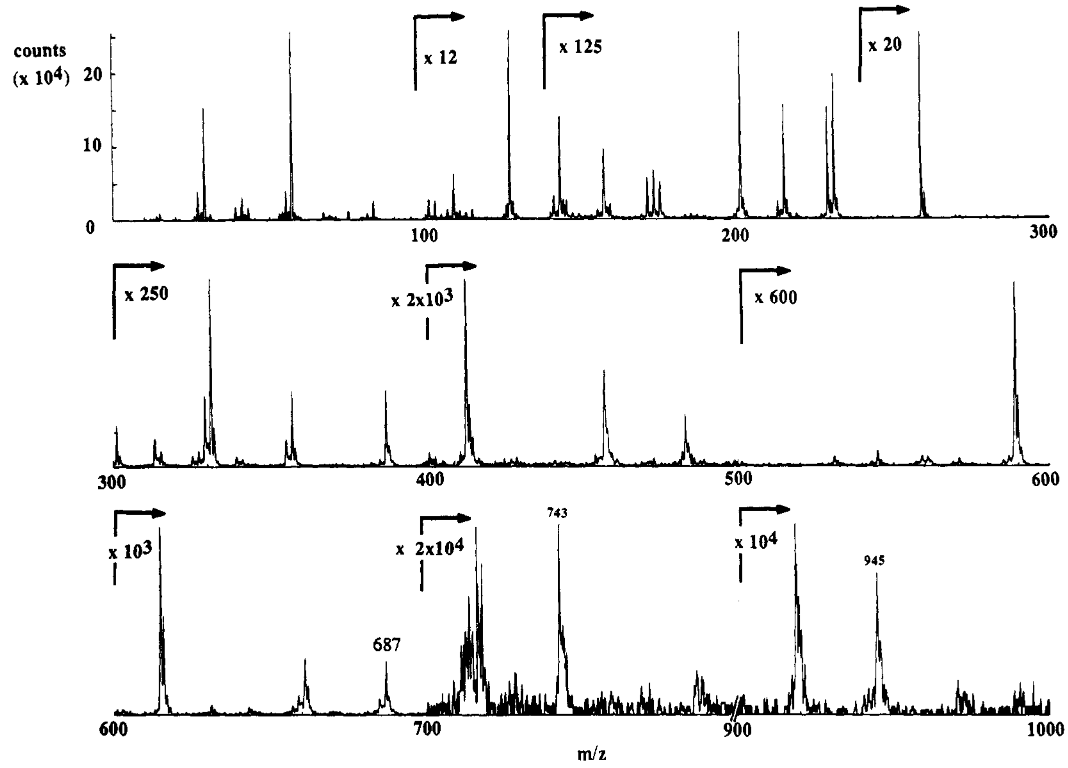

Figure 3. Positive ion ToF-SIMS spectrum of polymer C.

Table VI
Major Cations and Tentative Structural Assignments for DETOSU + t-CDM/HD from ToF-SIMS Analysis of Polymers B and C in Figures 2, 3, and 5b,c

m/z	assignments
687/685	$(M_{DETOSU} + M_{HD})(M_{DETOSU} + M_{CDM}) \pm H$
743	$(M_{DETOSU} + M_{HD})(M_{DETOSU} + M_{CDM}) + (C{=}O)CH_2CH_3$
945	$(M_{DETOSU} + M_{HD})(M_{DETOSU} + M_{CDM}) + 259^a$
1017	$(M_{DETOSU} + M_{CDM})(M_{DETOSU} + M_{HD})_2 + H$
1043	$(M_{DETOSU} + M_{CDM})_2(M_{DETOSU} + M_{HD}) + H$
1275	$(M_{DETOSU} + M_{CDM})(M_{DETOSU} + M_{HD})_2 + 259^a$
1301	$(M_{DETOSU} + M_{CDM})_2(M_{DETOSU} + M_{HD}) + 259^a$
1373	$(M_{DETOSU} + M_{CDM})_2(M_{DETOSU} + M_{HD})_2 + H$
1399	$(M_{DETOSU} + M_{CDM})_3(M_{DETOSU} + M_{HD}) + H$

[a] The 259 component is derived from DETOSU (see text).

trum of polymer A in Figure 1. In the main, general structures may be assigned to the ions in Figure 4 for polymer D, which are very similar to that observed for polymer A, i.e., $(X \pm H)^+$, $(X - O \pm H)^+$, $(X - C_2H_5)^+$, and $(X + (C{=}O)CH_2CH_3)^+$, where X is a combination of one or more DETOSU and HD monomer units. This suggests that there is a common mechanism of ion formation for all the polymers A–D, where the major fragmentation of the polymer backbone takes place in the vicinity of the orthoester functional group.

Cations Diagnostic of DETOSU + HD/t-CDM. A number of significant ions are detected for polymers B and C in Figures 2 and 3 and in the high mass range, in Figure 5b,c, which are absent in the positive ion spectrum of polymers A and D. These cations are of low intensity, but possible structures may be assigned to ions containing both diols and the DETOSU unit(s) as shown in Table VI.

Semiquantitative Analysis of t-CDM and HD Levels. From the preceding discussion, diagnostic ions specific to the DETOSU, t-CDM, and HD units have been identified. By comparison of their relative peak area intensities, these ions may be employed to estimate the surface content of t-CDM and HD, relative to their respective bulk concentrations. Figure 6 shows the comparison of the peak areas, *A*, of the *m/z* 109 (diagnostic of t-CDM), 101 (diagnostic of HD), and 127 (diagnostic of DETOSU) peaks as a function of nominal polymer composition. Peak areas than peak heights were chosen for the analysis because each peak in the secondary ion spectrum is defined over a number of rather than one spectral channels. It is evident that there is a near-linear relationship between the $A_{109}/A_{109} + A_{127}$ ratio and the bulk t-CDM levels. The slight deviation from linearity at high t-CDM levels may be attributable to the small but significant contribution of the $(M_{CDM}H)^+$ ion to the *m/z* 127 signal with increasing bulk t-CDM composition. For HD, the ratio $A_{101}/A_{101} + A_{127}$ also shows a linear increase with increasing HD bulk composition in Figure 6. These data suggest that the peak areas of the ions within this mass range reflect the nominal bulk composition in a quantitative manner.

Negative Ion ToF-SIMS. No differences were observed in the negative ion ToF-SIMS spectra of all the polymer series examined. Anion signals observed in the *m/z* 100–1000 range were extremely weak for the entire poly(orthoester) series and were of little additional diagnostic value. Figure 7 shows the negative ion ToF-SIMS (*m/z* 0–100) for polymer A. The *m/z* 73 ion is the major anion within the *m/z* 0–100 region and may be assigned to $CH_3CH_2COO^-$ formed from the cleavage of the orthoester bonds.

General Comments. The XPS and ToF-SIMS analysis of this series of poly(orthoesters) provides a detailed insight into the surface chemistry of these novel polymeric biomaterials. The data presented in this report are of significant value both from a biomedical perspective and also as a useful addition to the XPS and SIMS literature on polymer surface analysis.

From the surface analysis viewpoint, the XPS data allow the quantitative assessment of the surface chemical state of the poly(orthoesters). The ability to identify the orthoester functionality will be particularly relevant in future planned studies on the surface hydrolysis of these polymers on exposure to biological fluids. The detailed consistent fragmentation patterns observed within the ToF-SIMS spectra also draw particular interest. The detection of

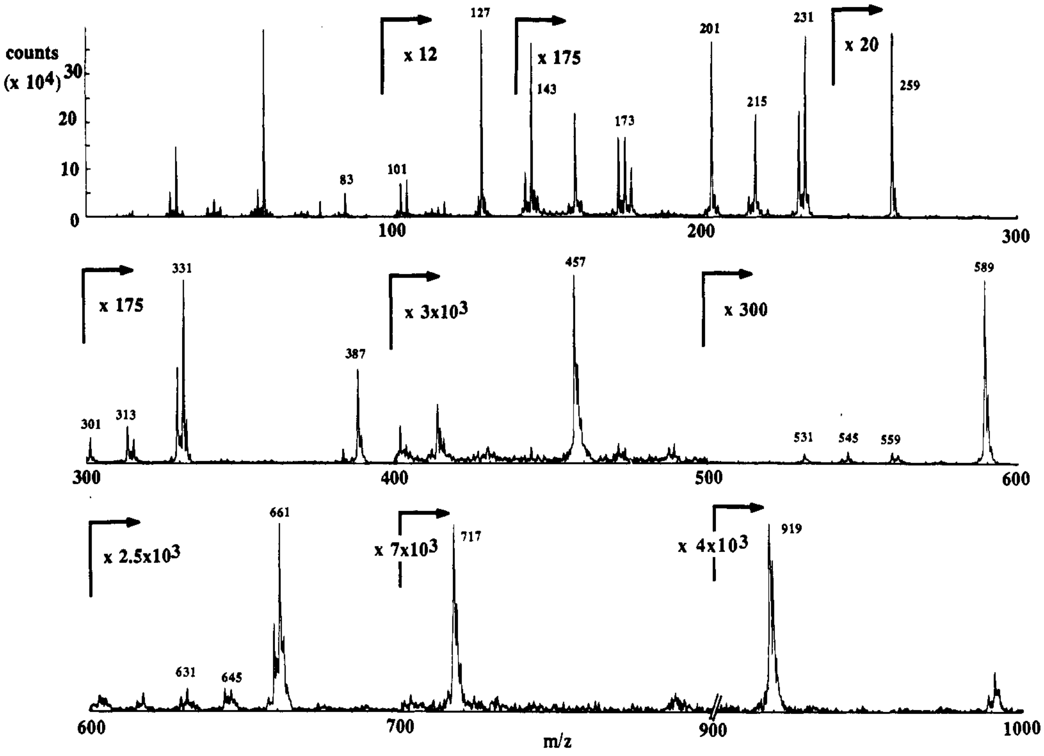

Figure 4. Positive ion ToF-SIMS spectrum of polymer D.

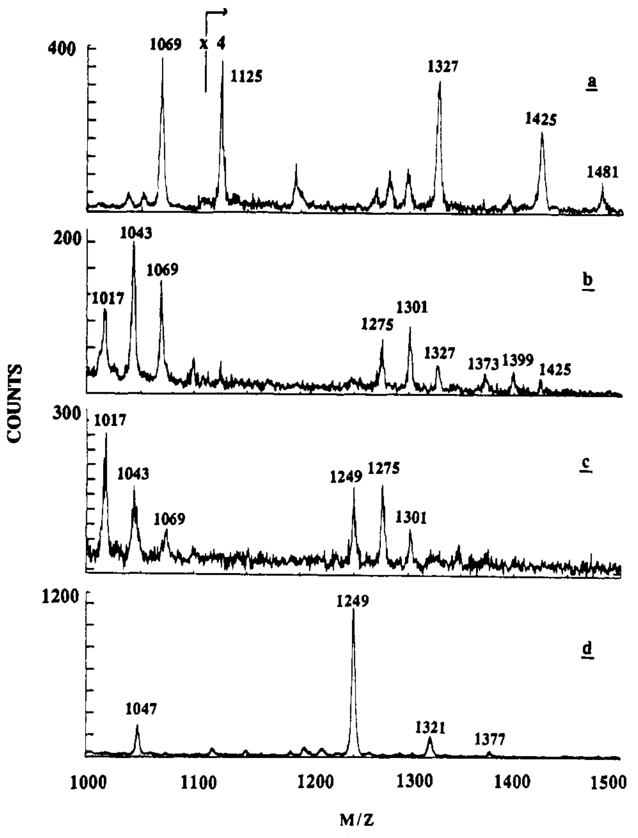

Figure 5. Positive ion ToF-SIMS spectrum (m/z 1000–1500) for (a) polymer A, (b) polymer B, (c) polymer C, and (d) polymer D.

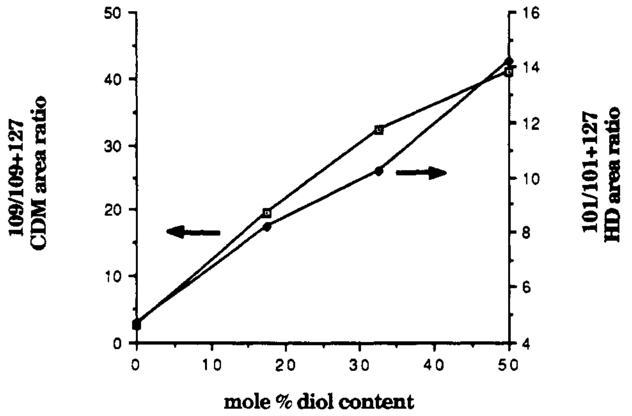

Figure 6. Graph of the area ratios of signals diagnostic of HD (m/z 101), t-CDM (m/z 109), and DETOSU (m/z 127) as a function of bulk polymer composition.

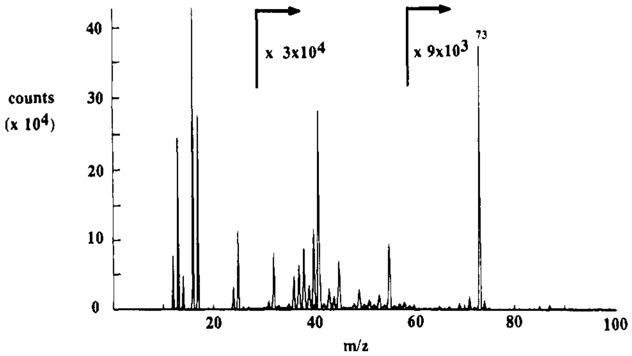

Figure 7. Negative ion ToF-SIMS spectrum of polymer A.

cations and/or anions that may be assigned to M ± H is emerging as a common feature in polymer SIMS spectra. Despite the complexity of the poly(orthoester) structure, the ToF-SIMS data may be readily interpreted to distinguish ions diagnostic of each type of repeat unit and also ions specific to the diads and triads arising from the random copolymer sequence. From the above assignments, it is evident that the major fragmentation of the polymer backbone occurs within the region of the ether linkage for the diols and also at the orthoester functional group for DETOSU. In the case of these poly(orthoesters), it is interesting to speculate on the nature of the fragmentation of the polymer since the cleavage of the orthoester bonds may involve the exocyclic or the endocyclic alkoxy group. Hence, two discrete series of fragments are possible.

The exocyclic cleavage of the orthoester functional group may give rise to the formation of the $(M_{DETSOU} \pm H)^+$,

Scheme I

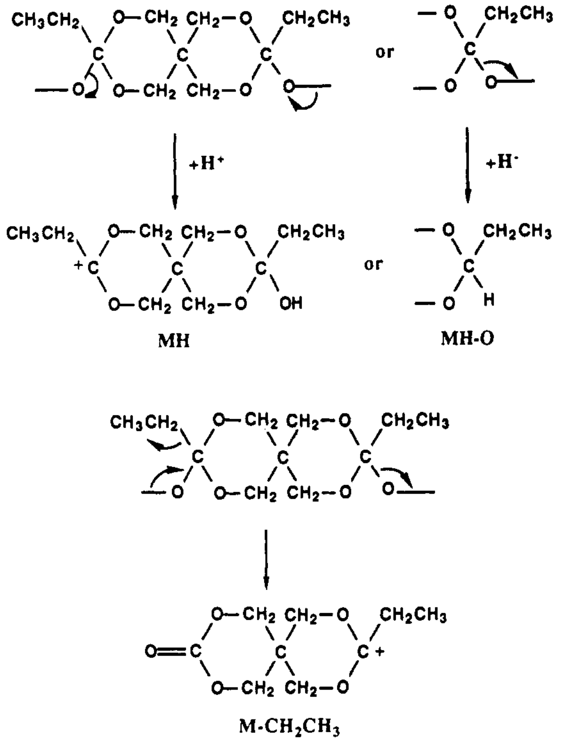

Scheme II

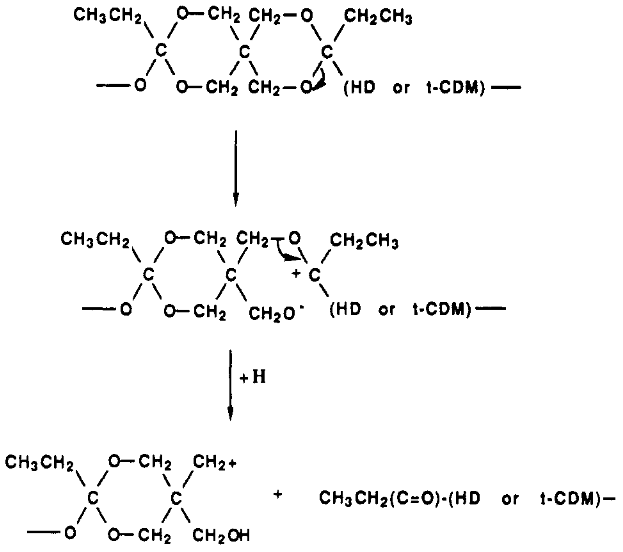

$(M_{DETOSU} - O \pm H)^+$, and $(M_{DETOSU} - CH_2CH_3)^+$ ions as shown in Scheme I. Conversely, endocyclic cleavage of the orthoester bonds gives rise to the (Y or X + $(C{=}O)CH_2CH_3)^+$ ions. A possible mechanism of ion formation may be that shown in Scheme II. The cations diagnostic of DETOSU at *m/z* 127, 143, 157, 159, 173, and 175 and the anion at *m/z* 73 also arise from the cleavage of the endocyclic alkoxy bonds.

The excellent correlation between ToF-SIMS ion peak areas and bulk composition for the diols is also noteworthy. Similar observations have been observed for hard and soft segment models in polyurethanes,[15] in the sequencing of poly(alkyl/hydroxyalkyl methacrylate) copolymers,[24] and for nylon copolymers.[25] Despite concerns over the influence of the matrix effects on ion yields, a significant body of work is emerging in the literature that suggests that SIMS analysis of polymers may be undertaken in a semiquantitative manner, albeit under carefully controlled experimental conditions.

From a biomedical standpoint, the surface analysis data confirm the purity of the surface structure, a prerequisite for any potential clinical application. The ability to differentiate the different chemical functionalities within the surface structure of the poly(orthoester) with SIMS and XPS provides not only a detailed insight into the polymer interfacial structure but also the foundation work for future research, designed to examine the mechanism and loci of surface degradation during the hydrolysis of the copolymer. These studies are in progress.

Acknowledgment. R.A.P.L. thanks the Science and Engineering Research Council (SERC) for a postgraduate studentship, and M.C.D. acknowledges the SERC for awarding a project grant for the surface analysis research.

References and Notes

(1) Heller, J. *Crit. Rev. Ther. Drug Carrier Syst.* **1984**, *1*, 39.
(2) Holland, S. J.; Tighe, B. J.; Gould, P. L. *J. Controlled Release* **1986**, *4*, 155.
(3) Leong, K. W.; Brott, B. C.; Langer, R. *J. Biomed. Mater. Res.* **1985**, *19*, 941.
(4) Heller, J.; Penhale, D. W. H.; Helwing, R. F. *J. Polym Sci., Polym. Lett. Ed.* **1980**, *18*, 82.
(5) Heller, J.; Fritzinger, B. K.; Ng, S. Y.; Penhale, D. W. H. *J. Controlled Release* **1985**, *1*, 225.
(6) Heller, J.; Fritzinger, B. K.; Ng, S. Y.; Penhale, D. W. H. *J. Controlled Release* **1985**, *1*, 233.
(7) Heller, J.; Penhale, D. W.; Fritzinger, B. K.; Rose, J. E.; Helwing, R. F. *Contracept. Delivery Syst.* **1983**, *4*, 43.
(8) Briggs, D. *Surf. Interface Anal.* **1986**, *9*, 391.
(9) Briggs, D. In *Polymer Surfaces and Interfaces*; Feast, W. J., Munro, H. S., Eds.; John Wiley: Chichester, U.K., 1987; p 33.
(10) Briggs, D. *Br. Polym. J.* **1989**, *21*, 3.
(11) Davies, M. C.; Lynn, R. A. P. *Crit. Rev. Biocompat.* **1990**, *5*(4), 297.
(12) Briggs, D. In *Comprehensive Polymer Science*; Book, C., Price, C., Eds.; Pergamon Press: New York, 1989; p 543.
(13) Davies, M. C.; Short, R. D.; Khan, M. A.; Watts, J. F.; Brown, A.; Eccles, A. J.; Humphrey, P.; Vickerman, J. C.; Vert, M. *Surf. Interface Anal.* **1989**, *14*, 115.
(14) Davies, M. C.; Wilding, I. W.; Melia, C. D.; Brown, A. *J. Appl. Polym. Sci.* **1990**, *39*, 1827.
(15) Hearn, M. J.; Ratner, B. D.; Briggs, D. *Macromolecules* **1988**, *21*, 2950.
(16) Davies, M. C.; Khan, M. A.; Watts, J.; Paul, A.; Domb, A.; Langer, R. *J. Appl. Polym. Sci.* **1991**, *42*, 1597.
(17) Bletsos, I. V.; Hercules, D. M.; Greifendorf, D.; Benninghoven, A. *Anal. Chem.* **1985**, *57*, 2384.
(18) Bletsos, I. V.; Hercules, D. M.; van Leyen, D.; Benninghoven, A. *Macromolecules* **1987**, *20*, 407.
(19) Sherwood, P. M. A. In *Practical Surface Analysis by Auger and X-ray Photoelectron Spectroscopy*; Briggs, D., Seah, M. P., Eds.; Wiley-Interscience: New York, 1985; p 445.
(20) Eccles, A. J.; Vickerman, J. C. *J. Vac. Sci. Technol.* **1989**, *A7*, 234.
(21) Briggs, D.; Hearn, M. J. *Vacuum* **1986**, *36*, 1005.
(22) Pijpers, A. P.; Donners, W. A. B. *J. Polym. Sci., Polym. Chem. Ed.* **1985**, *23*, 453.
(23) Davies, M. C.; Lynn, R. A. P.; Watts, J. F.; Paul, A. J.; Heller, J., in preparation.
(24) Briggs, D.; Ratner, B. D. *Polym. Commun.* **1988**, *29*, 6.
(25) Briggs, D. *Org. Mass Spectrom.* **1987**, *22*, 91.
(26) Leggett, G. J.; Briggs, D.; Vickerman, J. C. *J. Chem. Soc., Faraday Trans.* **1990**, *86*, 1863.
(27) Leggett, G. J.; Vickerman, J. C.; Briggs, D. *Surf. Interface Anal.* **1990**, *16*, 3.

Registry No. A (copolymer), 134680-98-1; A (SRU), 134680-99-2; B (copolymer), 88849-65-4; D (copolymer), 88849-64-3; D (SRU), 134681-00-8.